Available online at www.sciencedirect.com

SCIENCE DIRECT®

Catalysis Today 109 (2005) 167–177

CATALYSIS TODAY

www.elsevier.com/locate/cattod

Investigation of the mechanism of sediment formation in residual oil hydrocracking process through characterization of sediment deposits

Anthony Stanislaus [a,*], Andre' Hauser [b], Mina Marafi [a]

[a] *Petroleum Refinery Department, Petroleum Research and Studies Center,*
Kuwait Institute for Scientific Research, P.O. Box 24885, Safat, Kuwait
[b] *Central Analytical Laboratories, Kuwait Institute for Scientific Research, P.O. Box 24885, Safat, Kuwait*

Abstract

In deep conversion of petroleum residues by hydrocracking, the refiners often face the problem of sediment or sludge formation, which causes equipment fouling and catalyst deactivation and leads to enormous financial burden in terms of increased costs of operation, maintenance and shutdown. The primary objective of the present study was to obtain information on the composition and structure of the sediments and to understand the mechanism of their formation. Two samples of coke-like sediments, one collected from an industrial vacuum residue hydrocracking unit, and the other produced in pilot plant experiments with the same industrially used feedstock (VR from Kuwait export crude), were analyzed by chemical analysis as well as by various other techniques, such as TGA, NMR, and FT-IR. Prior to analyses, the sediments were fractionated by sequential extraction with heptane, toluene, and tetrahydrofuran. Structural characterization of the sediment material showed the presence of a variety of polyaromatic structures with different degrees of condensation and alkyl substitution. Presentations of average molecular structures were constructed for a number of fractions, such as heptane soluble (HS, 38 wt.%), heptane insoluble–toluene soluble (HIS–TS, 31 wt.%) and tetrahydrofuran insoluble (THFIS, 28 wt.%), separated from the pilot plant sediment. The HIS–TS fraction contained a modified asphaltene-like material. It was more aromatic and contained shorter aliphatic chains than the asphaltenes obtained from VR. The presence of a large amount of HIS–TS modified asphaltenes in the pilot plant sediment suggests that asphaltenes play a key role in the initial stage of sediment formation. The industrial sediment, which underwent severe cracking and condensation reactions on prolonged exposure to high temperature conditions, was highly carbonized (THFIS, 82 wt.%).

Keywords: Residue hydroconversion; Sludge formation; Asphaltenes deposition; Coke formation

---

1. Introduction

The crude oil production and refining trends worldwide indicate that the crude available to the refiners are becoming heavier and dirtier, producing large quantities of heavy oil fractions and residues during distillation in the refineries. The oil industry is under increasing pressure to convert residues to distillates and, more importantly, to increase their capacity for light and middle distillates production as well as to improve their quality in accordance with the new specifications, due to deteriorating crude oil quality and stringent product specifications.

The refiners use various processes for converting the low value residues to more valuable transportation fuels. Two routes, namely, carbon rejection and hydrogen addition, are commonly used for residual oil conversion and upgrading [1–3]. The hydrogen addition route has the advantage over the carbon rejection route when the quality of the distillate products is considered. The distillates produced by the hydroconversion process have lower levels of sulfur, nitrogen, aromatics and other contaminants and have better stability and can easily meet the stringent specifications imposed by environmental regulations. Consequently, deep conversion of heavy petroleum oils and residues to lighter cuts by hydroconversion has gained considerable importance in recent years.

One of the problems faced by the refiners in residual oil hydrocracking at high conversion is the formation of soft coke-like substances called sediment or sludge [4,5]. The carbonaceous sediment materials usually deposit on the reactor and downstream vessels as well as on the catalyst surface and cause both operability and rapid catalyst deactivation problems. The

---

[*] Corresponding author.
E-mail address: astanis@prsc.kisr.edu.kw (A. Stanislaus).

0920-5861/$ – see front matter © 2005 Elsevier B.V. All rights reserved.
doi:10.1016/j.cattod.2005.08.014

deposits usually accumulate in the downstream separators, heat exchangers and fractionating towers and foul the transfer lines, eventually causing a shutdown [6,7]. Equipment fouling by the coke-like sediments formed in residual oil hydroconversion or the hydrocracking process can lead to enormous financial burdens in terms of increased costs of operation, maintenance and shutdown. The refiners often use chemical and mechanical treatments to remove the deposits from the equipment [8]. Some refiners use antifoulant chemical additives to the feed to suppress the formation of sediments [9,10].

The problem of sediment formation and equipment fouling becomes particularly more serious at high operating temperatures when the conversion of residues to distillates is high and exceeds 60%. To minimize operability problems caused by the formation and deposition of sediments in residue hydrocracking processes, the refiners are often forced to operate at low conversion levels. Formation of sediments is, thus, a critical factor that limits the maximum attainable conversion in commercial residue hydroprocessing units. Prevention or suppression of coke-like sediment materials is highly desirable to attain high conversion in residue hydroprocessing/hydrocracking operations.

Despite the fact that sediment formation affects the process economics significantly in residual oil hydroprocessing by limiting the conversion of residues to distillates and by increasing maintenance costs through equipment fouling, it has not received much attention and the mechanism of its formation is not fully understood. Prevention or mitigation of sediment formation is therefore of great interest. Measures to alleviate or suppress such deposit formation could be implemented in a more systematic and efficient way if the factors that influence sedimentation are identified. The mechanism of sediment formation and fouling should also be clearly understood for controlling them efficiently.

Factors influencing the formation of coke-like sediments during hydrocracking of heavy petroleum residues have been the subject of some investigations in this laboratory [11,12]. In our previous studies [13,14] attention was paid to understand the role of asphaltenes and operating severity in sediment formation. The effect of adding aromatic rich gas oils as diluents to vacuum residue (VR) feed on various conversions as well as on sediment formation was reported by us in a recent paper [15].

In the present study two samples of coke-like sediments, one collected from an industrial VR hydrocracking unit, and the other (fresh sediment) collected during pilot plant hydroprocessing experiments with the same industrially used feedstock, were analyzed and characterized by different analytical techniques. The primary objective of the study was to obtain information on the composition and structural characteristics of the sediment deposits and to understand the mechanism of their formation.

2. Experimental

2.1. Material

Two samples of coke-like sediments were the subject of the present study. One was obtained from the stripper bottom of the H-oil unit in Kuwait's National Petroleum Company's (KNPC's) refinery and the other one, fresh sediment, was produced in pilot plant experiments (collected from the high pressure separator) with the same feedstock as used in the refinery. Prior to analysis the sediments were fractionated by multiple extractions according to Scheme 1. Four fractions: (i) *n*-heptane soluble (HS); (ii) heptane insoluble–toluene soluble (HIS–TS); (iii) toluene insoluble–tetrahydrofuran soluble (TIS–THFS); and (iv) THF insoluble (THFIS), were obtained from the sediments. The solvent defined fractions were characterized by elemental analysis (EA), metal analysis (MA), molecular weight (MW) as well as various other techniques, such as thermo gravimetric analysis (TGA), Fourier transform infrared spectroscopy (FT-IR) and nuclear magnetic resonance spectroscopy (NMR).

2.2. Pilot plant experiments and analyses

A fixed-bed reactor system (manufactured by Vinci Technology, France; total volume: 242 ml, internal diameter: 11.9 cm) was used for hydrocracking of VR from Kuwait

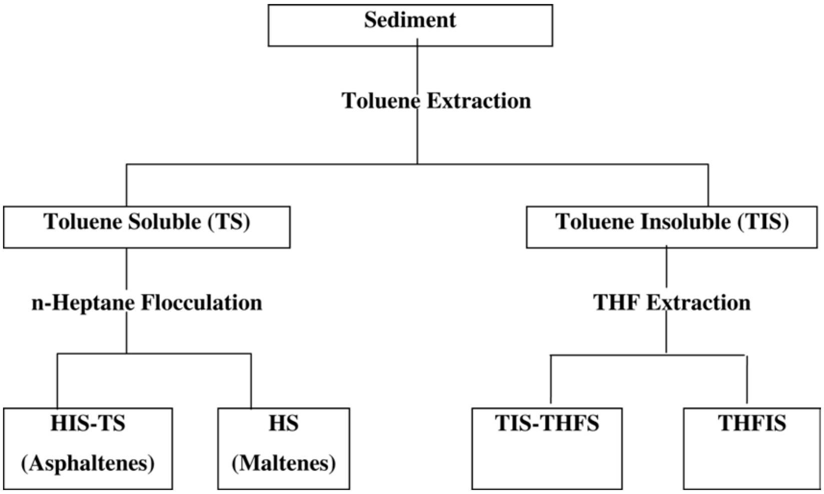

Scheme 1. Extraction scheme for sediments.

export crude (KEC). The feedstock characteristics and operating procedures were reported in detail elsewhere [15]. The feedstock contained 5.2 wt.% S, 0.44 wt.% N, 113 ppm V, 30 ppm Ni, 7.5 wt.% asphaltenes, and 18.5 wt.% CCR. This feed is the same as that used in the industrial unit. The operating conditions were: pressure, 135 bar; LHSV, 1 h^{-1}; H_2/oil ratio, 1000; temperature, 440 °C.

- *EA*. The C, H, N and S contents of the sediments were determined in an elemental analyzer from CARLO ERBA INSTRUMENTS (Model EA 1110 CHNS). Each sample was analyzed in duplicates.
- *MA*. The metals (Ni, Mo, Al, Fe and V) were determined by inductively coupled plasma optic emission spectroscopy (ICP-OES) using a JOBIN-YVON instrument (JY-24) with double order grating and nitrogen purge. The spectra ranged from 160 to 800 nm. The metal quantification is based on calibration curves established with matrix matched standards.
- *MW*. A vapor pressure osmometer (KNAUER, model K-7000) was used to determine the MW of the sediment fractions.
- *TGA*. The analyses of approximately 30 mg of sample placed in a macro platinum cell were carried out on a SHIMADZU TGA-50. The analyses were run in the temperature range from 30 to 1000 °C with a heating rate of 10 °C/min in an air and nitrogen atmosphere. The flow rate of the gases was 50 ml/min.
- *FT-IR*. The spectra of solid samples (2 mg in 40 mg KBr) and liquid ones (thin layer on KBr disk) were recorded using an FT-IR spectrometer from BRUKER (VECTOR 22). For each spectrum (400–4000 cm^{-1}) 32 scans were accumulated with 2 cm^{-1} resolution. The spectra were plotted in % transmittance.
- *NMR*. All NMR measurements were carried out on a BRUKER AMX 300 spectrometer (7.0463 T) equipped with a cross polarization/magic angle spinning (CP/MAS) accessory and a fully automated pneumatic unit for sample spinning.
    - *^{13}C solid-state NMR*. ^{13}C solid-state NMR spectra were obtained from original sediments and its THFIS fractions. The spectra of dried and ground samples were measured using proton gated decoupled single pulse excitation at high MAS (SPE/MAS) [16] and cross polarization with polarization inversion at low or moderate MAS (CP/PI/MAS) [17]. For more details see Hauser et al. [18]. As moderate MAS, 4 kHz (7 mm rotor) was chosen to minimize overlapping between the main signals (aliphatic and aromatic carbon) and the spinning side bands (SSB). Fifteen kilohertz (4 mm rotor), as high MAS, reduced the SSB to approximately 3% of the center signal and moved them to the margins of the spectral range.
    - *^{1}H, ^{13}C liquid-state NMR*. The soluble fractions were dissolved in $CDC1_3$ (99.8%) and tetramethylsilane (TMS) from WILMAD was used as internal standard for the ^{1}H NMR measurements. The ^{13}C chemical shift values were referred to the central signal of the $CDC1_3$ at 77.7 ppm. For ^{1}H NMR the sample concentration was approximately 15 wt.% in 0.5 ml $CDC1_3$. The solution was filled into a 5 mm tube and one drop of TMS was added. To obtain quantitative ^{13}C NMR spectra, the solution was transferred into a 10 mm tube, and the concentration was increased to about 60 wt.% Cr (acac)3 (Fluka) was also added to give a 0.1 M solution.

      ^{1}H NMR spectra were acquired with a spectral width of 5.5 kHz, a pulse angle of 90° (20 μs) and a delay time of 3 s using the single pulse excitation (SPE) technique. The corresponding settings for the quantitative ^{13}C NMR measurements were: spectral width: 25 kHz, pulse angle: 45° (6 μs) and delay time: 20 s. The pulse sequence used was SPE with inverse gated ^{1}H decoupling.

3. Results

3.1. EA/MA

The elemental analysis data for the original industrial and pilot plant sediment samples are presented in Table 1. The elemental composition of asphaltenes in the VR feed is also included in the table for comparison. The results indicate appreciable differences, between the industrial and pilot plant sediments. The pilot plant sediment is rich in hydrogen and has a remarkably higher H/C ratio. In addition, it has a very low metal (V, Ni, Mo, Al and Fe) content compared with the industrial sample (Table 1).

The presence of metals, such as Mo, Ni, V and Al, in the industrial sediment sample indicates that some catalyst fines carried over from the reactor along with the effluents are associated with the deposits. The industrial sediment deposits contain about 3.6 wt.% iron. It is likely that the iron is coming

Table 1
Elemental and metal analysis data of sediments and VR asphaltenes

Sample	Elemental analysis (wt.%)[a]				H/C	Metals (wt.%)[b,c]				
	C	H	N	S		V	Ni	Mo	Fe	Al
Industrial sediment	82.89	4.05	1.08	5.73	0.59	0.52	0.24	0.3	3.6	1.6
Pilot plant sediment	83.05	7.07	0.87	6.65	1.02	0.03	0.02	ND	0.12	0.03
VR-asphaltenes of KEC	83.90	7.80	1.10	7.20	1.12	0.04	0.01	ND	ND	ND

[a] Relative standard deviation: C, 1.7%; H, 0.9%; N, 1.7%; S, 2.1%.
[b] Relative standard deviation: 5%.
[c] ND = not detected.

Table 2
Yields of solvent defined sediment fractions

Fraction	Amount (wt.%)	
	Industrial sediment	Pilot plant sediment
HS	16	38
HIS–TS	<1	31
TIS–THFS	1	3
THFIS	82	28
Recovery	99	100

from corrosion of the reactor vessels, pipelines and downstream equipment since the feed does not contain any noticeable amount of iron. The fresh sediment collected from pilot plant experiments closely resembles the VR asphaltenes in their elemental composition. Their H/C ratio is slightly lower than that of asphaltenes, but much larger than that of the industrial sediment sample.

The sediments were separated into different fractions by multiple extractions with different solvents (Scheme 1). Four fractions (i) HS, (ii) HIS–TS, (iii) TIS–THFS and (iv) THFIS, were obtained from the deposits by solvent extraction. The percentages of the different fractions recovered from the two sediment samples are presented in Table 2.

The industrial sediment sample contained a substantially large percentage (>80 wt.%) of THFIS material. The amount of the HIS–TS material, which represents the asphaltenes and modified asphaltenes with large polynuclear aromatic (PNA) cores in the deposits, was very low (<0.5 wt.%). The amount of TIS–THFS fraction that represents the coke precursors was also relatively low (1–2 wt.%) in the industrial sediment sample. The pilot plant sediment sample, on the other hand, consisted of 38 wt.% HS maltenes, 31 wt.% HIS–TS asphaltenes, 3 wt.% coke precursors (TIS–THFS) and 28 wt.% insoluble residue (THFIS).

Table 3 presents the elemental composition of the different fractions separated from the fresh sediment collected in pilot plant experiments. The HS maltene fraction contains the highest H/C ratio, whereas the TIS–THFS fraction and the THFIS residue have much lower H/C ratios. Interestingly, the H/C ratio of the HIS–TS fraction has an H/C ratio value that is slightly lower than that of feed asphaltenes. The concentrations of sulfur, nitrogen and metals (V and Ni) in this fraction are also lower than that of feed asphaltenes. The last two fractions, which represent the coke precursors and coke, have low H/C ratios, indicating that they are highly aromatic.

Table 4
Weight loss percentages in different temperature region during TGA of pilot plant sediment and its solvent defined fractions

Temperature range (°C)	Weight loss under N_2 (wt.%)			
	Sediment	HS	HIS–TS	THFIS
25–200	0.3	0.8	2.3	0
200–300	1.3	5.1	6.6	0
300–400	4.3	15.5	10.6	0.2
400–500	21.1	59.2	24.8	2.0
500–600	5.7	4.7	5.3	3.2
600–700	1.0	0.3	1.3	2.2
700–800	0.2	0	0.8	1.1
800–1000	3.4	0.6	3.1	3.2
Total	37.3	86.2	54.8	11.9

The presence of a large amount of HIS–TS asphaltenes or modified asphaltenes in the fresh sludge/sediment collected in the pilot plant experiments suggests that asphaltenes play a key role in sediment formation. The high concentration of insoluble residues in the industrial sediment sample indicates that this material contains primarily coke. The low concentration of asphaltenes in the industrial sediment sample compared with the pilot plant one suggests that the coke might have been formed through the successive transformation of asphaltenes to coke precursors and then to coke by dehydrogenation, cracking, condensation, and carbonization reactions during prolonged stay in the equipment after deposition. The presence of large amounts (>80 wt.%) of THFIS coke-like material with low H/C ratio (0.6) in the industrial sediment is consistent with this.

Further characterization of the sediment material produced in the pilot plant experiments and its solvent-extracted fractions by TGA, IR and NMR techniques was done to gain information about their volatility and structural characteristics.

3.2. TGA

The volatility of the sediment formed in pilot plant experiments and its solvent-extracted fractions (HS, HIS–TS, THFIS) was determined by measuring the weight loss as a function of temperature up to 1000 °C in a thermo gravimetric analyzer. The weight loss percentages during heating in nitrogen atmosphere in different temperature regions are presented in Table 4.

Table 3
Elemental, metal and molecular weight analysis data of solvent defined sediment fractions from pilot plant sediment

Fraction	Elemental analysis (wt.%)[a]				H/C	Metals (wt.%)[b,c]					MW
	C	H	N	S		V	Ni	Mo	Fe	Al	
HS	84.2	9.9	0.4	5.4	1.42	0.01	ND	ND	0.02	0.01	600
HIS–TS	86.8	7.3	0.9	5.0	1.01	0.03	0.01	ND	0.02	0.01	1050
TIS–THFS	88.5	5.8	1.1	4.6	0.78	NA	NA	NA	NA	NA	NA
THFIS	88.7	4.1	1.1	5.5	0.55	0.03	0.08	ND	0.48	0.02	NA

[a] Relative standard deviation: C, 1.7%; H, 0.9%; N, 1.7%; S, 2.1%.

[b] Relative standard deviation: 5%.

[c] ND = not detected, NA = not analyzed.

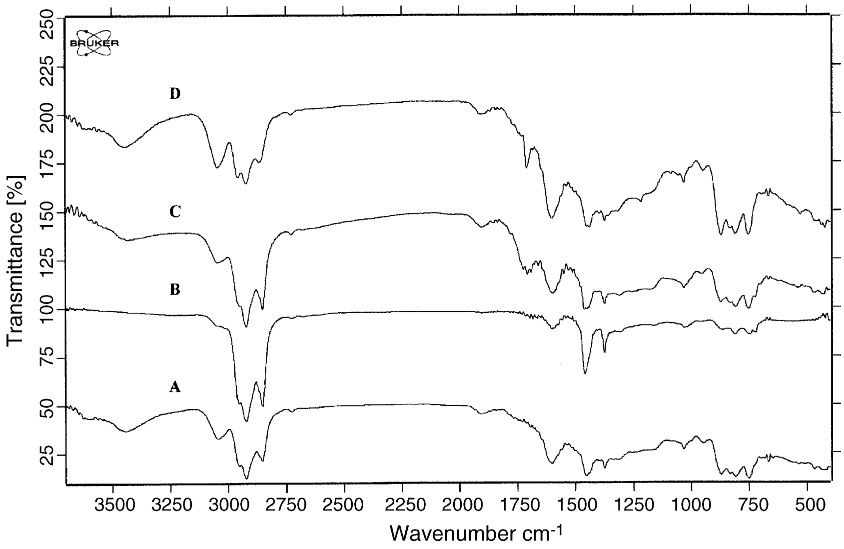

Fig. 1. FT-IR spectra of the pilot plant sediment (A) and its solvent defined fractions; HS (B), HIS–TS (C) and THFIS (D).

It is seen that for the original sediment, 37.3 wt.% of the volatile materials present in the sediment are removed during heating in a nitrogen atmosphere. The remaining 62.75 wt.% of the material is non-volatile. The maximum weight loss (31.1 wt.%) occurs in the 300–600 °C region. The weight loss at temperatures below 300 °C is very small (<2 wt.%). The results indicate that a significant part of the sediment is sufficiently volatile to boil in the range of heavy gas oil (HGO). In the case of the HS portion, about 75 wt.% weight loss occurs in the temperature region 300–500 °C during heating in a nitrogen atmosphere (Table 4), indicating that this fraction consists of mainly volatile materials boiling in the HGO range. Another 5 wt.% of the material present in this fraction is removed at a slightly higher temperature (500–600 °C). About 14 wt.% of the material in this extract is non-volatile, even up to 1000 °C. The three regions of weight loss in the TGA indicate the presence of different types of materials with varying molecular weights.

The HIS–TS fraction contains less volatile material than the HS fraction (Table 4). About 45 wt.% of the material is non-volatile and left as residue when heated in a nitrogen atmosphere. The maximum volatilization (40.7 wt.%) occurs between 300 and 600 °C, indicating the presence of a large amount of material boiling in the HGO range. It is likely that this fraction contains a substantial amount of asphaltenes with bulky PNA cores formed during the hydrocracking process. A certain amount of polycondensed large non-volatile asphaltenic material also appears to be present in this fraction.

In the THFIS residue, a major portion (>88 wt.%) is non-volatile (Table 4). The volatile portion (about 12 wt.%) appears to be relatively heavy, requiring temperatures in the range 400–1000 °C for their removal.

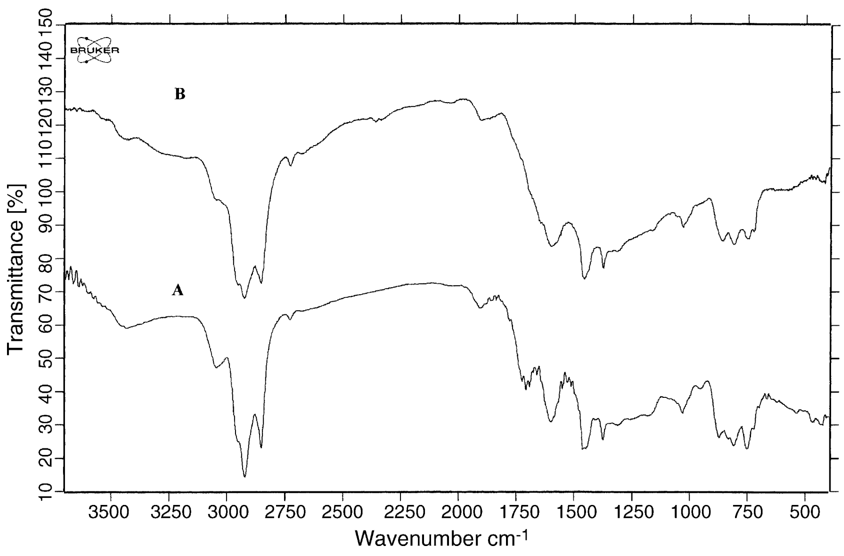

Fig. 2. FT-IR spectra of the HIS–TS fraction of pilot plant sediment (A) and a VR asphaltene (B).

3.3. FT-IR

The sediment material collected from pilot plant tests and its solvent-fractionated components were analyzed by FT-IR. The FT-IR spectra are demonstrated in Fig. 1. Major transmission bands identified along with the functional groups causing them are presented in Table 5. Comparing the different fractions, the spectra show some variations in the signal intensity of the functional groups. For example, the HS fraction has a high content of aliphatic CH (C–H modes at 2900, 1460 and 1375 cm^{-1}) and a small amount of aromatic CH (C–H modes at 3100 and 800 cm^{-1}) and C,C double bonds (C=C modes at 1600 cm^{-1}). For the HIS–TS (asphaltenes) and THFIS (residue) fractions, the aromatic C–H and C=C modes become the dominating features of the IR spectra, indicating that these fractions consist mainly of condensed PNAs. The intensity ratio of the asymmetric CH_3 (2965 cm^{-1}) and CH_2 (2925 cm^{-1}) modes clearly show that the aliphatic chains become shorter from the HS fraction towards the residue (see Fig. 1 and Table 5, last column).

In Fig. 2, the spectra of a VR asphaltene and the HIS–TS fraction are shown together. The resemblance between the spectra is obvious; both show clearly transmission bands assigned to aromatic C–H and C=C groups, The striking similarity between the HIS–TS fraction and VR asphaltenes clearly indicate that asphaltenes are involved in the formation of sediments. The intensity ratio of the asymmetric CH_3 to CH_2 modes, however, differs for both samples.

3.4. NMR

NMR has become a powerful tool for structural characterization of solid carbonaceous deposits [16,19] and liquid hydrocarbons [20]. In liquid and solid-state NMR, for example, different types of structural entities can be identified and quantified [20].

Therefore, the liquid extracts (HS, HIS–TS and TIS–THFS) were further characterized by ^{1}H and ^{13}C NMR to examine the distribution of carbon and hydrogen according to various structural groups found in aliphatic and aromatic moieties [21–24]. As for the pilot plant-produced sediment sample and its THFIS residue solid-state ^{13}C NMR was applied.

Fig. 3 shows the solid-state ^{13}C NMR spectra of the original sediment sample and its THFIS residue. Peaks of aromatic carbon (100–170 ppm) and aliphatic carbon (0–70 ppm) are indicated in these spectra.

Based on the NMR measurements, aromatic and aliphatic carbon as well as hydrogen was identified and the percentages of H and C in different structural entities were estimated for the pilot plant sediment and its solvent defined fractions. The results are compiled in Table 6.

3.5. Average molecular structure

The molecular structures of sediments or sludge materials produced in heavy oil conversion processes are poorly understood and information on their structural characteristics

Table 5
Functional group analysis obtained from FT-IR of pilot plant sediment and its solvent defined fractions

Sample	Functional groups[a]									Ratio CH_3 to CH_2
	CH Arom. (870–730 cm^{-1})	C–O–C, C–O–H (1307, 1158, 1033 cm^{-1})	C–H Sat. (1460, 1375 cm^{-1})	C=C Arom. (1600 cm^{-1})	C=O (1710 cm^{-1})	CH aldehyde (2728 cm^{-1})	CH Sat. (2955, 2925, 2850 cm^{-1})	CH Arom. (3025 m^{-1})	NH/OH (3300 cm^{-1})	
Sediment	+++	++	++	++	+	+	+++	++	+	0.77
HS	+	–	++	+	–	–	+++	+	–	0.60
HIS–TS	+++	+++	++	++	+++	+	+++	++	–	0.66
THFIS	++++	+++	++	+++	+	+	++	+++	+++	0.93

[a] Arom. = aromatic; Sat. = saturated.

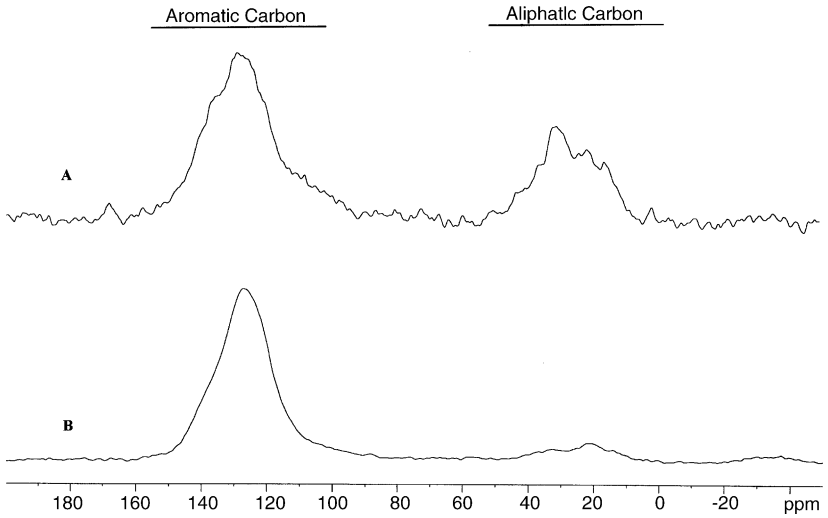

Fig. 3. Solid-state SPE/MAS ^{13}C NMR spectra of the pilot plant sediment (A) and its THFIS residue (B).

are scarce. In the present study we have made an attempt to propose average molecular structures by combining data deduced from NMR, EA and MW determinations. The parameters used to construct a structural presentation are listed in Table 7. The average MW of the two soluble fractions, e.g., HS and HIS–TS, were determined by VPO method in our laboratory. The values were 600 and 1050 Da for HS and HIS–TS fractions.

The structural parameters of the three fractions, HS, HIS–TS and THFIS, are presented in the first column of Tables 7–9. Based on these parameters in conjunction with MW data it is possible to construct a hypothetical molecule [25] that matches best the analytical results. The average molecule combines all typical, structural features of the solvent defined fractions. Some caution should be applied while describing a structural diverse material like sediments by only a single average structure. The construction of hypothetical structures, however, makes it possible to visualize differences in the chemical nature between the fractions.

Table 6
^{1}H and ^{13}C NMR results of pilot plant sediment and its solvent defined fractions

Parameter[a]	Percentage of H and C in structural entities[b]			
	Sediment	HS	HIS–TS	THFIS
H_{al}	NA	91	81	NA
$H_{al};\gamma$	NA	13	10	NA
$H_{al};\beta$	NA	48	36	NA
$H_{al};\alpha$	NA	30	35	NA
H_{ar}	NA	9	19	NA
C_{al}	31	61	34	11
C_{ar}	69	39	66	89
C_{ar};H	38	NA	NA	53
C_{ar};H,b3	NA	16	36	NA
C_{ar};q	31	27	47	37
C_{ar};b3	5	NA	NA	2
C_{ar};b2,n,CH_3	16	NA	NA	18
C_{ar};R	10	7	7	12
C_{ar};X	1	0	1	1

[a] Description of parameters see Table 7. C_{ar};H,b3: tertiary and triple bridged aromatic C; C_{ar};b2,n,CH_3: aromatic C in double-bridged-head position, next to a naphthenic rings or a CH_3-group.

[b] NA = not analyzed.

3.5.1. HS fraction

The average molecule of the HS fraction, which is demonstrated in Fig. 4, has in the core a pyrene structure surrounded by aliphatic groups. A closer look at the structural parameters reveals that the carbon numbers of the aromatic substructure and the total aliphatic carbon number satisfy well the experimental data (Table 7).

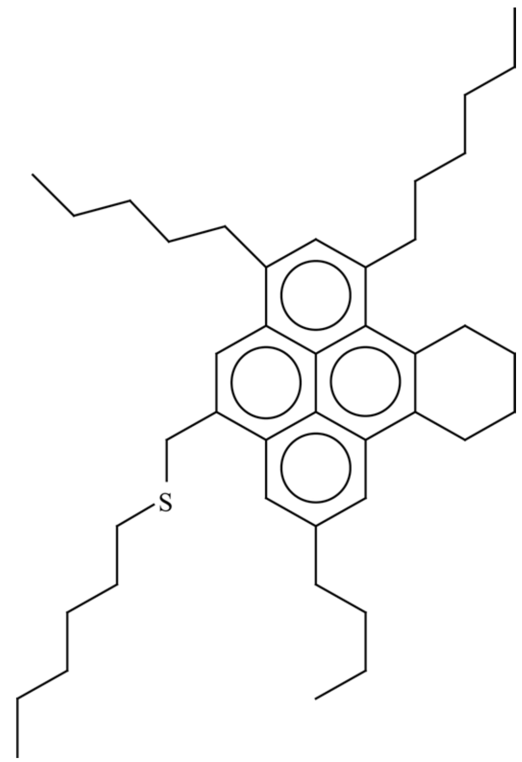

Fig. 4. Average molecular structure presentation of HS fraction from pilot plant sediment.

Table 7
Comparison between analytical data and average molecular structure for the HS fraction of pilot plant sediment

Parameter	Definition	Data	
		Analytical	Structural
C	Carbon atoms	42	42
H/C	Hydrogen–carbon ratio	1.41	1.43
S	Sulfur atoms	1	1
N	Nitrogen atoms	0	0
MW	Molecular weight	600	596
CAR	Aromatic carbon	16	16
CAR;H	Tertiary aromatic carbon	5	4
CAR;b3	Triple bridged aromatic carbon	2	2
CAR;b2	Double bridged aromatic carbon	0	4
CAR;sub	Substituted aromatic carbon, except b3, b2, X	9	6
CAR;R	Alkyl substituted aromatic carbon, except CH_3	3	4
CAR;X	Aromatic carbon attached to heteroatoms	0	0
CAL	Aliphatic carbon	26	26
CAL;*t*-CH_3	Aliphatic carbon in CH_3	4	4
$CH_2CH(\mathit{CH_3})CH_2$	Aliphatic carbon in CH_3 branches	1	0
$CH_2\mathit{CH}(CH_3)_2$	Aliphatic carbon in terminal branching position	1	0
H	Hydrogen atoms	59	60
HAR	Aromatic hydrogen	5	4
HAL	Aliphatic hydrogen	54	56
HAL;α	Aliphatic hydrogen in α position to aromatic ring	18	12 + 2[a]
HAL;β	Aliphatic hydrogen in alkyl chains or naphthenic rings	28	30
HAL;γ	Aliphatic hydrogen in terminal CH_3	8	12
fa	Aromaticity = CAR/C	0.38	0.37
γ	Condensation = (CAR;b3 + CAR;b2)/CAR	0.13	0.38
σ	Substitution = CAR;sub/(CAR;H + CAR;sub)	0.64	0.60

[a] HAL;α + –S–$\mathit{CH_2}$–CH_2.

Table 8
Comparison between Analytical data and average molecular structure for the HS–TIS fraction of pilot plant sediment

Parameter[a]	Data			
	Analytical	Structural		
		55% A + 45% B	A	B
C	76	77	50	110
H/C	1.01	1.01	0.92	1.12
S	2	2	1	3
N	1	0	0	1
MW	1050	1057	678	1521
CAR	50	51	32	75
CAR;H	15	14	8	21
CAR;b3	12	10	8	13
CAR;b2	11	15	8	24
Car;sub	11	12	8	16
CAR;R	5	6	4	8
CAR;X	1	0	0	1
CAL	26	26	18	35
CAL;*t*-CH_3	7	4	4	4
$CH_2CH(\mathit{CH_3})CH_2$	1	1	1	0
$CH_2\mathit{CH}(CH_3)_2$	1	1	1	1
H	77	66	46	91
HAR	15	14	8	21
HAL	62	52	38	70
HAL;α	27	15	12	18
HAL;β	28	26	14	41
HAL;γ	8	12	12	11
fa	0.66	0.66	0.64	0.68
γ	0.46	0.50	0.50	0.49
σ	0.42	0.47	0.50	0.43

[a] Description of parameters see Table 7.

Table 9
Comparison between analytical data and average molecular structure for the THFIS residue of pilot plant sediment

Parameter[a]	Data	
	Analytical[b]	Structural
C	739	684
H/C	0.56	0.58
S	17	24
N	8	12
MW	≈10000	9540
CAR	658	648
CAR;H	392	312
CAR;b3	15	36
CAR;n,b2,CH_3	133	156
CAR;b2	NA	144
CAR;CH_3	NA	12
CAR;R	89	132
CAR;X	7	12
CAL	81	36
H	410	396
HAR	392	312
HAL	18	84
fa	0.89	0.95
γ	NA	0.28
σ	NA	0.32

[a] Description of parameters see Table 7.

[b] NA = not analyzed.

3.5.2. HIS–TS fraction

The HIS–TS fraction, which represents asphaltenes and coke precursors, can be considered as an intermediate phase, which possesses a lower H/C ratio compared to maltenes but a clearly higher one than the residue. As for the aromaticity, the HIS–TS fraction stands also between the other two fractions, HS and residue, as indicated by the NMR data. TGA under nitrogen showed that 55 wt.% of the HIS–TS fraction is volatile at temperatures below 600 °C. Recent studies [26] on the MW distribution of asphaltenes by laser desorption mass spectrometry (LD-MS) have revealed a bimodal MW distribution with maxima around 600 and 1700 amu for asphaltenes of an Arabian crude oil. Thus, for calculating the average molecule, we have divided the HIS–TS fraction into two hypothetical structures, which represent the two extremes in molecular weight, one volatile sub-fraction (A) with about 700 Da and another more refractory one (B) with about 1500 Da. Since both fractions fall into the same solubility class, we have assumed that both structures, A and B, differ merely in the size but not in their chemical nature. Fig. 5A and B exhibit these two structures and Table 8 lists the average structural parameters for A and B and for the combination of A and B with a weighing of 55% A and 45% B. The resemblance of the combined structural parameters with the ^{13}C analytical data is satisfactory (Table 8). Especially the high number of double and triple bridged aromatic carbons is well reflected by the two structures.

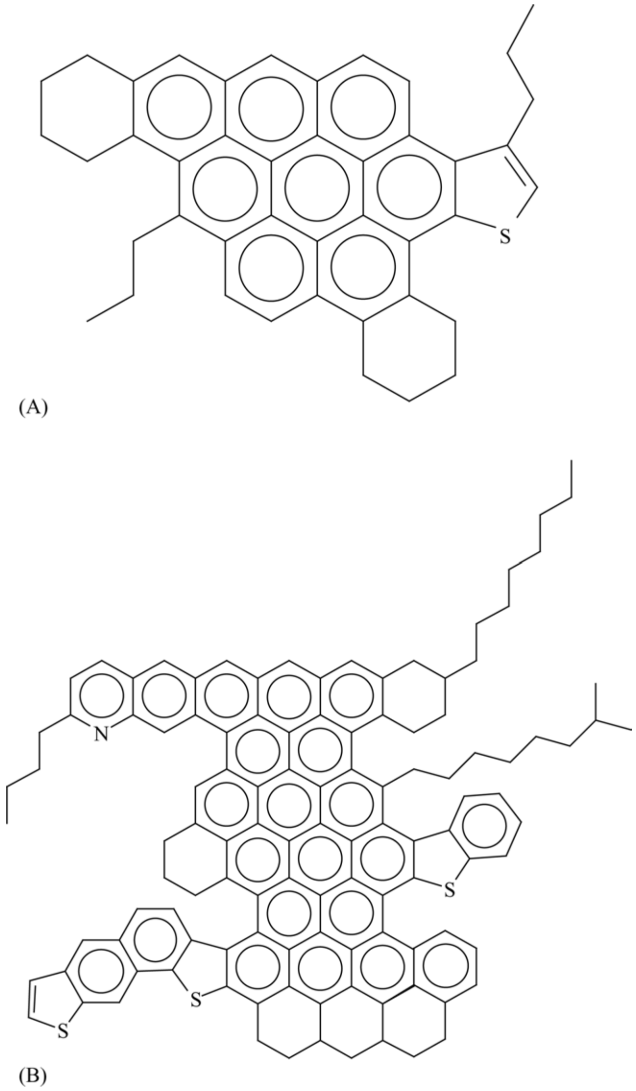

Fig. 5. (A) Average molecular structure presentation of 55% HIS–TS fraction from pilot plant sediment. (B) Average molecular structure presentation of 45% HIS–TS fraction from pilot plant sediment.

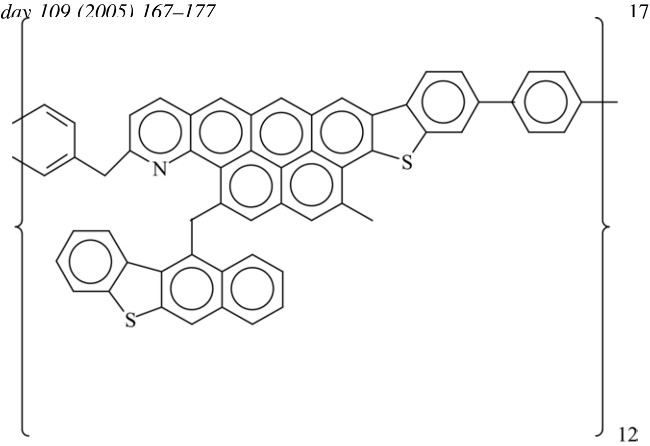

Fig. 6. Average molecular structure presentation of TFHIS residue from pilot plant sediment.

3.5.3. THFSI residue

The THFIS residue contains coke-like molecules, which can be broken down to highly aromatic substructures. These substructures are repeatedly joined by short saturated carbon chains forming large polyaromatic hydrocarbon sheets, which are combined in clusters [27–29]. Typically, the material posses a remarkable low H/C ratio (<0.6) combined with a very high aromaticity (fa > 0.8). The average substructure constructed and presented in Fig. 6 fulfills these requirements. The number of substructures joined depends on the MW assumed, but the structural characteristics of each subunit match the obtained NMR and EA results. The corresponding average structural parameters are presented in Table 9.

4. Discussion

The results of chemical analysis and detailed characterization of the sediment produced during VR hydrocracking in pilot plant tests indicate the following. The sediment contains mainly organic materials, and a large percentage of the materials are sufficiently volatile to boil in the same range as HGO. A large portion (about 70 wt.%) of the sediment is soluble in various solvents. It has much higher hydrogen content than coke. About 30 wt.% of the sediment contains asphaltene-like material that is insoluble in heptane, but soluble in toluene. IR analysis of the sediment material showed the presence of asphaltene-like material in the sediment. The asphaltene separated from the sediment contained shorter aliphatic chains and was more aromatic than the asphaltenes in the VR feedstock. Fractionation and structural characterization of the sediment material by

NMR analysis showed the presence of a variety of PNA structures with different degrees of condensation and alkyl substitution.

Many previous investigators have observed sediment or dry sludge formation in various processes, such as thermal cracking, visbreaking and hydrocracking that are used for the conversion of heavy petroleum residues into distilled products [7,19,30]. Different mechanisms have been proposed in these earlier studies to explain sediment formation.

Sediments are soft carbonaceous materials. They are produced in the catalytic and thermal processes at high conversion levels under severe operation conditions. Many early workers [31,32] suggested that sediments are coke precursors or incompletely polycondensed coke and postulated mechanisms involving a sequence of cracking and condensation steps. Coke and coke-like sediments may also be formed when reaction intermediates, such as unstable radicals produced by thermal cracking, are reconstituted into high molecular weight PNAs. Initiation of free radical polymerization occurs more easily at high temperature conditions. Highly unsaturated fluids or cracked stocks are especially susceptible to this type of polymerization.

Many workers have correlated the formation of sediments and coke deposits in petroleum residue conversion processes with asphaltenes in residue [33,34]. Storm et al. [19] observed a large decrease in the amount of sediments formed in the liquid product during hydroconversion of VR when the HIS asphaltenes were removed from the feed. It has been suggested that sediments are formed because the asphaltenes precipitate during processing. Sludge and deposit formation due to asphaltene flocculation have been reported during the production, transportation, storage and treatment of crude oils [35,36].

Residue oils usually contain high concentrations of asphaltenes and CCR. The solubility of asphaltenes in oil is limited. Asphaltenes are soluble in aromatic and polar solvents and insoluble in paraffinic substrates. The resin components of the residual oil are highly aromatic and they act as a solvent or dispersing agent for the asphaltenes. The oil fraction of the residues is less polar and contains mainly saturated hydrocarbons, with a high H/C ratio. It is proposed that the asphaltenes remain dispersed in the less polar oil medium due to the presence of resins [37–40] and a residual oil can be considered as a colloidal system. The micelles of the dispersed phase contain asphaltene and resins.

During hydrocracking of residual the oils, both the non-asphaltenic phase and the asphaltenes undergo chemical changes. The oils and resins are cracked and hydrogenated at a faster rate than the asphaltenes. As a result, the aromaticity and the solvent power of the resin phase decreases. At the same time, reactions involving scission of side chains and cracking of naphthenic rings occur in the asphaltene molecules leaving the PNA core unaffected. These changes make the product oil (effluent) more saturated and the unconverted asphaltene cores remaining in the product more aromatic and condensed than those in the feed. Consequently, a disturbance in the asphaltene's adsorption/solubility equilibrium in the resin-oil medium occurs leading to the precipitation of asphaltenes as sediments.

This was confirmed by Bartholdy and Anderson [41] by a study on product oil stability by flocculation onset titration procedure after severe hydrotreatment. Presence of hard core asphaltenes with increased aromaticity in H-oil process effluents and their role in sediment formation was demonstrated recently by Robert et al. [42].

The fresh sediment produced in our pilot plant experiments contained a large amount of HIS–TS material. It is possible to assume that this soft HIS–TS sediment consists essentially of asphaltene cores separated from the product during the reaction, as Wiehe [38] suggested. The HIS–TS material contained 55 wt.% volatile compounds boiling in the range of HGO. Its, average molecular weight was 1050 Da. It is likely that it is composed of heavy PNA molecules and modified asphaltenes, together with a small amount of polycondensed PNAs. The material resembled closely asphaltenes in its chemical and structural characteristics, but contained lower hydrogen content and alkyl substituents, indicating partial side-chain cleavage to leave the asphaltenes with large PNA cores.

The solubility and volatility data indicate the presence of a variety of materials with different solubility and volatility in the pilot plant sediment. It is likely that a part of the sediment contains wax-like paraffinic material and low molecular weight PNAs with long side chains and naphthenic rings. This portion is predominantly soluble in heptane. The other portion appears to be composed of modified asphaltenes (HIS–TS), coke precursors (THFS) and coke (THFIS). It appears that condensation, oligomerization and polymerization of aromatic structures (i.e., asphaltene cores) have occurred, to a limited extent, to form coke precursors and coke with large PNA entities during the process.

The sediment deposits collected from the stripper column of an industrial residue hydrocracking unit (KNPC's H-oil unit) contained mostly THFIS coke. It is likely that these deposits originated from precipitated asphaltene cores which underwent further condensation and polymerization reactions on prolonged exposure to high temperature conditions, resulting in highly condensed coke-type structures. Fouling of the other downstream equipment, such as heat exchangers and pipelines, could also result from asphaltene precipitation. Generation and separation of high molecular weight PNAs could also be partly responsible for fouling. Carryovers of these precipitated sediment materials into the down stream equipment by the liquid phase could result in continuous deposition and coking over a long period of time, resulting in the buildup of carbonaceous deposits that could lead to equipment fouling.

5. Conclusions

In the present study, two samples of coke-like sediment deposits, one collected from an industrial vacuum residue (VR) hydrocracking unit and the other collected during pilot plant experiments with the same feedstock (VR from Kuwait export crude) were analyzed by various analytical techniques. The fresh sediment from pilot plant experiments closely resembled the asphaltenes from VR in their elemental composition. The H/

C ratio (0.98) was slightly lower than that of the asphaltenes (1.11), but much higher than that of the industrial deposit (0.59). A large percentage of the pilot plant sediment was sufficiently volatile to boil in the same range as heavy gas oil. Structural characterization of different solvent extracts from the pilot plant sediment, such as the heptane soluble (HS, 38 wt.%) and the heptane insoluble–toluene soluble (HIS–TS, 31 wt.%) fractions as well as well as the tetrahydrofuran insoluble (THFIS, 28 wt.%) residue, by IR and NMR showed the presence of a variety of polyaromatic structures with different degrees of condensation and alkyl substitution. Combining NMR, elemental analysis and molecular weight data, average molecular structures were constructed. The HIS–TS fraction contained a modified asphaltene-like material. It was more aromatic and contained shorter aliphatic chains than the asphaltenes obtained from VR. Its molecular weight was also lower than that of the petroleum asphaltenes. The industrial sediment, which underwent severe cracking and condensation reactions on prolonged exposure to high temperature conditions, was highly carbonized and contained low levels of volatile and soluble matter (<20 wt.%).

The presence of a large amount of HIS–TS modified asphaltenes in the pilot plant sediment suggests that asphaltenes play a key role in the initial stage of sediment formation. Our results provide direct evidence to the general proposition that sediment formation in residual oil conversion processes is caused by asphaltene insolubility and incompatibility in the product oils.

Acknowledgements

The authors are highly thankful to the KFAS management for its financial support of the project and acknowledge the cooperation and assistance of KNPC Shuaiba refinery in providing the vacuum residue feedstock and H-oil unit sediment samples. The authors would also like to thank Ms. M. Behbehani, Ms. H. Abdullah and Ms. A. Al-Adwani of the Central Analytical Laboratory of KISR for their assistance in sediment characterization. The authors deeply appreciate the assistance of pilot plant hall staff for their assistance in experiments aimed to produce fresh sediment samples with the vacuum residue feedstock. Finally, the authors would like to express their deepest gratitude to Dr. M. Absi-Halabi for his useful discussions during the course of the work.

References

[1] M.R. Gray, Upgrading of Petroleum Residue and Heavy Oil, Marcel Dekker, New York, 1994.

[2] J.F. LePage, Residual and Heavy Oil Processing, Editions Technip, Paris, 1992;
P. Leprince, Petroleum Refining: Conversion Processes, Editions Technip, Paris, 2001.

[3] M.R. Khan, D.J. Patmore, in: J.G. Speight (Ed.), Petroleum Chemistry and Refining, Heavy Oil Upgrading Processes, Marcel Dekker, New York, 1998, p. 149.

[4] W.I. Beaton, R.J. Bertolacini, Catal. Rev. Sci. Eng. 33 (1991) 281.

[5] M.A. Bannayan, H.K. Lemke, W.K. Stephenson, Stud. Surf. Sci. Catal. 100 (1996) 273.

[6] M. Embaby, in: Proceedings of the Ketjen Catalyst Symposium on KNPC H-Oil Unit Performance, Kurhaus, The Netherlands, 25–28 May, 1986.

[7] H.K. Lemke, W.K. Stephenson, Petrol. Sci. Technol. 16 (1998) 335.

[8] B.C. Groce, Oil Gas J. 29 (1996) 81.

[9] S.S. Shih, D. Dellart, J. VanVooren, H.D. Harbs, S. Baggott, Controlling bed fouling of hydrotreators, in: Proceedings of the Third International Conference on Refinery Processing, AIChE Spring Meeting, Atlanta, USA, March, 2000.

[10] T.C. Xiao, J.X. Su, H.T. Wang, Y.L. Lu, Z.F. Yan, A.P.E. York, J.B. Claridge, J. Sloan, M.L.H. Green, Ind. Eng. Chem. Res. 39 (2000) 3679.

[11] A. Stanislaus, A. Al-Barood, M. Maeafi, A. Hauser, Investigation of factors controlling sediment formation during catalytic hydrocracking of Kuwait vacuum residues, Final Report, KISR Publication No. 6450, Kuwait Institute for Scientific Research, 2002.

[12] A. Stanislaus, M. Absi-Halabi, Z. Khan, Stud. Surf. Sci. Catal. 100 (1996) 189.

[13] A. Stanislaus, M. Absi-Halabi, Z. Khan, in: M. Oballa, S.S. Shih (Eds.), Catalytic Hydroprocessing of Petroleum and Distillates, Fate of Asphaltenes During Hydroprocessing of Heavy Petroleum Residue, Marcel Dekker, New York, 1994, p. 159.

[14] M. Absi-Halabi, A. Stanislaus, F. Owaysi, Z. Khan, S. Diab, Stud. Surf. Sci. Catal. 53 (1990) 201.

[15] M. Marafi, A. Al-Barood, A. Stanislaus, Petrol. Sci. Technol. 27 (2005) 899.

[16] A. Fonseca, P. Zeuthen, J.B. Nagy, Fuel 75 (1996) 1363.

[17] X. Wu, K.W. Zilm, J. Magn. Reson. A 102 (1993) 205.

[18] A. Hauser, A. Stanislaus, A. Marafi, A. Al-Adwani, Fuel 84 (2005) 259.

[19] D.A. Storm, S.J. Decanio, J.C. Edwards, E.Y. Sheu, Petrol. Sci. Technol. 15 (1997) 77.

[20] L. Petrakis, D. Allen, NMR for Liquid Fossil Fuels, Elsevier, Amsterdam, 1987

[21] M.A. Callejas, M.T. Martinez, T. Blasco, E. Sastre, Appl. Catal. A 218 (2001) 181.

[22] D.A. Storm, J.C. Edwards, S.J. DeCanio, E.Y. Sheu, Energy Fuels 8 (1994) 561.

[23] S. Gillet, P. Rubini, J.J. Delpuech, J.C. Escalier, P. Valentin, Fuel 60 (1981) 221.

[24] D.J. O'Donnell, S.O. Sigle, K.D. Berlin, G.P. Sturm, J.W. Vogh, Fuel 59 (1980) 166.

[25] D.A. Storm, S.J. Decanio, E.Y. Sheu, in: M.K. Sharma, T.F. Yen (Eds.), Asphaltene Particles in Fossil Fuel Exploration, Recovery and Refining Processes, Sludge Formation During Heavy Oil Conversion, Plenum Press, New York, 1994, p. 81.

[26] R. Tanaka, S. Sato, T. Takanohashi, F.E. Hunt, R.E. Winans, Energy Fuels 18 (2004) 1405.

[27] J. Christopher, A.S. Sarpal, G.S. Kapur, A. Krishna, B.T. Tyagi, M.C. Jain, S.K. Jain, A.K. Bhatnagar, Fuel 75 (1996) 999.

[28] I. Schwager, P.A. Farmanian, J.T. Kwan, V.A. Weingerg, T.F. Yen, Anal. Chem. 55 (1983) 42.

[29] J.W. Shrokoff, M.N. Siddiqui, M.F. Ali, Energy Fuels 11 (1997) 561.

[30] J.F. Kritz, Can. J. Chem. Eng. 72 (1994) 85.

[31] M.E. Levinter, M.I. Medvedeva, G.M. Panchenko, Y.G. Aseev, Y.N. Nedoshivin, G.H. Finkelstein, M.F. Galiakbarov, Khim. Tekhol. Topl. Masel. (9) (1966) 31.

[32] M.E. Levinter, M.I. Medvedeva, G.M. Panchenko, G.L. Agapov, M.F. Galiakbarov, R.K. Galikeev, Khim. Tekhol. Topl. Masel. (4) (1967) 20.

[33] M. Absi-Halabi, A. Stanislaus, D.L. Timm, Appl. Catal. 72 (1991) 193.

[34] J.G. Speight, Catal. Today 98 (2004) 55.

[35] A. Chaala, B. Benallal, S. Hachelef, Can. J. Chem. Eng. 72 (1994) 1036.

[36] G.A. Mansoori, J. Petrol. Sci. Eng. 17 (1997) 101.

[37] I.A. Wiehe, K.S. Liang, Fluid Phase Equilib. 117 (1996) 201.

[38] I.A. Wiehe, Ind. Eng. Chem. Res. 32 (1993) 2447.

[39] J.G. Speight, in: S. Kaliaguine, Mahay (Eds.), Catalysis on the Energy Scene, Upgrading of Heavy Oils and Residua: The Nature of the Problem, Elsevier, Amsterdam, 1984, p. 515.

[40] J.G. Speight, ACS Div. Pet. Preprints 32 (1987) 413.

[41] J. Bartholdy, S.I. Anderson, Energy Fuels 14 (2000) 52.

[42] E.C. Robert, I. Merdrignac, B. Rebours, V. Harlie, S. Kressman, J. Coldier, Petrol. Sci. Technol. 21 (2003) 615.